

P5D.1 The precipitating Cloud System Studies Using UHF radar/Integrated Sounding System in Taiwan

Pay-Liam Lin and Hsin-Hung Lin
Department of Atmospheric Sciences, National Central University, Taiwan

1. Introduction

The NCU(National Central University) ISS (Integrated Sounding System) was deployed in Dongsha island during May 5 to June 25, 1998 for the SCSMEX and deployed in the southeastern coast of Taiwan during May 5 to June 30,2001 for the GIMEX. When Typhoon Nari made landfall over Taiwan, the ISS at the campus of NCU revealed a good observation. Several major convective events occurred in SCSMEX,GIMEX and Typhoon Nari will be discussed and compared in this investigation.

2. Distinguish the Precipitation Cloud System in SCSMEX

A time-height cross section of reflectivity, Doppler velocity and spectral width observed in the vertical beam of the 915 MHz profiler at Dong-Sha Island in SCSMEX on May 15, 1998 is shown in Fig. 1. The stratiform rain accompanied by a bright band in the equivalent reflectivity and a melting layer signature of rapidly accelerating hydrometeor fall speed below 4.5 km. Some heavier rain episodes illustrate deep convection and a mixture of deep convection with stratiform rain. Correlations between vertical radial velocity and range corrected signal power measured by the vertical pointing beam of 915 MHz radar wind profilers can be used to determine weather or not precipitation is present and what type of precipitation it is. The S-V correlation diagram on May 15, 1998 is shown in Fig. 2. Four major groupings of points can be identified including four representing conditions dominated by scattering from either air, rain, ice and melting ice.

The set of air is characterized by small radial vertical velocity and extends over a wide range of S/N values. This behavior is characteristic of Bragg scattering from air, where it appears that most of the vertical air motion measurement fall between $-0.3 \sim 1$ m/s. The set of ice is characterized by strong correlation between radial vertical velocity and S/N for values of $0 \sim -2$ m/s. The set of melting ice is a smaller set, it is characterized by strong S/N values(greater than 45 dB). The radial vertical velocity fall between -2 and -4 m/s. The set of rain is characterized by strong and large variability of radial vertical velocity and S/N values. This set of points has a slight correlation between vertical velocity and S/N value when compared with the other three sets.

In order to get a distinct separation between the cluster of points characteristics of those four categories, the radial vertical velocity histograms(Fig. 3) are plotted. There is distinct separation between the cluster of ice and those of air for larger values of vertical velocity. For smaller vertical velocity, however these two distributions merge. It seems we can find the range in vertical velocity approximately represents the optimum velocity threshold separating air and precipitation echoes.

3. Typhoon Nari revealed by Profiler Radar and Distrometer

The detailed velocity distribution associated with the convective systems of Typhoon Nari were revealed by the UHF radar Figure 4 illustrates the two-dimensional histograms of vertical velocity observed by ISS during a period of high rainfall rate, 11-12 LST, September 17 (Fig. 4a) and a period of low rainrate, 21-22 LST, September 17 (Fig. 4b). Because the radar reflectivity is sensitive to hydrometers, return echoes of the UHF radar are mainly contributed by the precipitation particles. In high-rainrate period, the histogram shows a clear separation around 4.5 km. Above 4.5 km, vertical velocities occur most frequently within the range of -2 ms⁻¹ to 2 ms⁻¹ with much more downward velocities than upward velocities, indicating the existence of prevailing frozen precipitating clouds and sporadic updrafts. Below 4.5 km, downward speed in the range of $5 - 8$ ms⁻¹ is dominant due to melting of solid particles to raindrops.

Comparing the histograms in low rainrate period (Fig. 4b) and high rainrate period (Fig.3a), a major difference is found below 5 km where downward motions in low rainrate period spread over a wider range with weaker magnitudes, implying that shallow convection and stratiform-type precipitation are dominant. There also exists clear-air echoes below 4.5 km in the low-rainrate period (Fig. 4b) as represented by higher counts of near zero velocity. It is also important to recognize that upward velocities above 5 km can reach about 2 ms⁻¹ during light rainfall period (Fig. 4b) and exceed 2 ms⁻¹ during high rainfall period (Fig. 4a).

The corresponding raindrop distribution measured by a 2-D video disdrometer is presented in Fig. 4c and 4d. During the high (low) rainfall period, the average raindrop size is 2 mm (1 mm) derived from the raindrop distribution in Fig. 4c (Fig. 4d) with maximum size about 4 mm (6 mm). However the number of raindrops during high rainfall period is one order of magnitude higher than that during light rainfall period. Since the terminal velocity of 2 mm and 1 mm raindrop is about 6.5 and 4 ms⁻¹, respectively, the disdrometer measurements are consistent with the vertical velocity measurements in the lower troposphere by UHF radar measurements.

Corresponding author address: Pay-Liam Lin,
Department of Atmospheric Sciences, National Central
University, Chung-Li 320, Taiwan
Tel.: +886-3-4223294 Fax:+886-3-4256841
Email: tliam@atm.ncu.edu.tw

Reference:

Ralph, F. M., P. J. Neiman, and D. Ruffieux, 1996: Precipitation Identification from Radar wind profiler spectral moment data: vertical velocity histograms, velocity variance and signal power vertical velocity correlations. J. Atmos. Oceanic Technol., 13, 545-559.

Sui, C.-H., C.-Y. Huang, Y.-B. Tsai, C.-S. Chen, Pay-Liam Lin, S.-L. Shieh, M.-H. Li, Y.-A. Liou, T.-C. Chen Wang, R.-S. Wu, G.-R. Liu, Y.-H. Chu et al, 2002: Typhoon Nari and Taipei Flood- A Pilot meteorology-hydrology Study. Submitted to EOS, Transactions

Williams, C. R., W. L. Ecklund, and K. S. Gage, 1995: Classification of precipitating clouds in the tropics using 915 MHz wind profilers. J. Atmos. Oceanic Technol., 12, 996-1012.

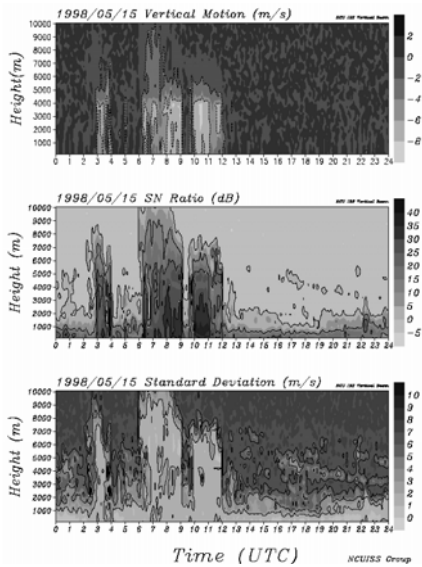


Fig.1, Time-height cross-sections of S/N, Vertical Velocity and standard deviation observed by the vertical beam of the 915MHz Profiler in SCSMEX, 15 May 1998.

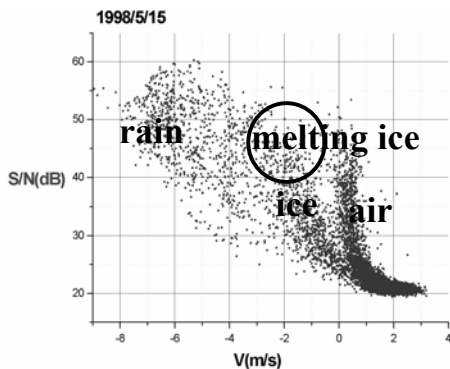


Fig.2, Scatterplot of Signal Power and vertical velocity measurements from the Vertically pointing beam of the 915MHz Profiler.

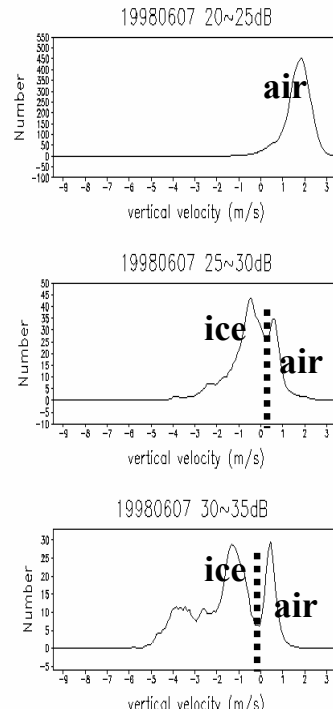


Fig.3, Histograms of vertical velocity in different Signal Power intervals. (a)20-25db (b)25-30db (c)30-35db.

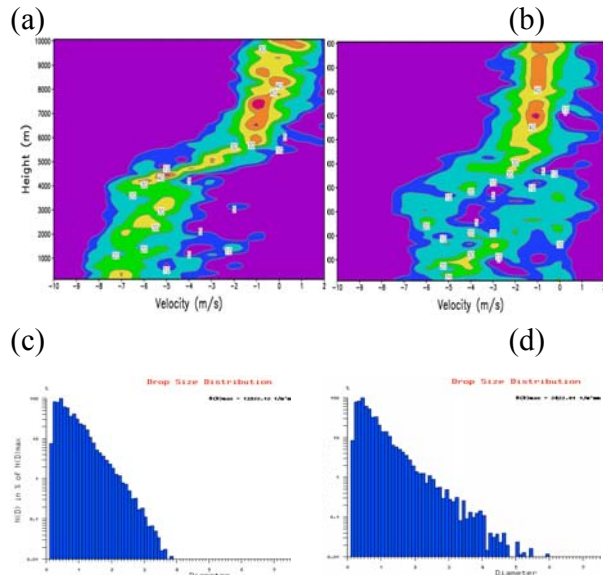


Fig. 4 Histograms of vertical velocity observed by ISS at NCU for (a) 11-12 LST, and (b) 21-22 LST, September 17, and the corresponding raindrop size distribution in (c) and (d) using a 2-D video.